

# Transactivation, Dimerization, and DNA-Binding Activity of White Spot Syndrome Virus Immediate-Early Protein IE1<sup>∇</sup>

Wang-Jing Liu,<sup>1</sup> Yun-Shiang Chang,<sup>2</sup> Hao-Ching Wang,<sup>3</sup> Jiann-Horng Leu,<sup>1</sup>  
Guang-Hsiung Kou,<sup>1\*</sup> and Chu-Fang Lo<sup>1\*</sup>

*Institute of Zoology, National Taiwan University, Taipei, Taiwan<sup>1</sup>; Department of Molecular Biotechnology, Da-Yeh University, Changhua, Taiwan<sup>2</sup>; and Institute of Biological Chemistry, Academia Sinica, Taipei, Taiwan<sup>3</sup>*

Received 16 June 2008/Accepted 20 August 2008

**Immediate-early proteins from many viruses function as transcriptional regulators and exhibit transactivation activity, DNA binding activity, and dimerization. In this study, we investigated these characteristics in white spot syndrome virus (WSSV) immediate-early protein 1 (IE1) and attempted to map the corresponding functional domains. Transactivation was investigated by transiently expressing a protein consisting of the DNA binding domain of the yeast transactivator GAL4 fused to full-length IE1. This GAL4-IE1 fusion protein successfully activated the *Autographa californica* multicapsid nucleopolyhedrovirus *p35* basal promoter when five copies of the GAL4 DNA binding site were inserted upstream of the TATA box. A deletion series of GAL4-IE1 fusion proteins suggested that the transactivation domain of WSSV IE1 was carried within its first 80 amino acids. A point mutation assay further showed that all 12 of the acidic residues in this highly acidic domain were important for IE1's transactivation activity. DNA binding activity was confirmed by an electrophoresis mobility shift assay using a probe with <sup>32</sup>P-labeled random oligonucleotides. The DNA binding region of WSSV IE1 was located in its C-terminal end (amino acids 81 to 224), but mutation of a putative zinc finger motif in this C-terminal region suggested that this motif was not directly involved in the DNA binding activity. A homotypic interaction between IE1 molecules was demonstrated by glutathione *S*-transferase pull-down assay and a coimmunoprecipitation analysis. A glutaraldehyde cross-linking experiment and gel filtration analysis showed that this self-interaction led to the formation of stable IE1 dimers.**

White spot syndrome virus (WSSV) is the causative agent of a disease that has led to severe mortalities of cultured shrimps all over the world (10, 14, 23, 53). WSSV is a large double-stranded DNA virus which is extremely virulent (23, 38, 39), has a wide host range (14, 33), and targets various tissues (32, 59). It was recently erected as the type species of genus *Whispovirus* in the family *Nimaviridae* (56). Although the complete sequence of the WSSV genome has been known for several years (7, 55, 60), knowledge of the biological functions of the viral proteins is still quite poor. The WSSV immediate-early gene *ie1* (31) was recently shown to use a shrimp signal transducer and activator of transcription (STAT) as a transcription factor to enhance its expression and contribute to its high promoter activity in host cells (30). In the present study, we further investigate the characteristics of WSSV IE1. This is made more difficult by the fact that no continuous shrimp cell line is currently available, and while bearing in mind that a heterologous system might introduce experimental artifacts, here we follow previous studies (22, 30, 34) and use the Sf9 insect cell system.

Many viral immediate-early genes encode multifunctional transcriptional regulators that both positively and negatively modulate gene expression (26, 52, 57). These transcriptional regulators must possess at least two functional domains, namely, a DNA binding domain (DBD) that allows attachment

of the transactivator to its target sequence within a gene promoter and a transactivation domain (TAD) that can interact with the basal transcription machinery and promote the transcription of the target genes. These two domains are often functionally independent and physically separate. In many cases, the activity of these transcriptional regulators is regulated by homophilic interactions (35, 42) as well as by the formation of heterodimers with other transcriptional factors. We show here that WSSV IE1 exhibits all three of these transcriptional regulator functions, and we also attempt to identify the domains that are associated with these functions.

While the DBDs are extremely well characterized both functionally and structurally, the activation domains do not share easily recognizable motifs or structures (54). Therefore, in the present study, the TAD of WSSV IE1 was investigated by analyzing the transient expression of GAL4 DBD-IE1 N- or C-terminal deletion mutants. IE1-DNA binding and the functionality of a previously identified Cys<sub>2</sub>/His<sub>2</sub>-type zinc finger DNA binding motif (31) were investigated using electrophoretic mobility shift assays (EMSAs). Finally, to investigate the intermolecular interactions of WSSV IE1, a combination of *in vitro* and *in vivo* assays were performed to test for IE1 homophilic interactions.

## MATERIALS AND METHODS

**Plasmids. (i) Luciferase effectors.** The plasmid pIZΔIE1/V5-His was used as a starting point in dual-luciferase reporter assays. It was modified from the commercialized plasmid pIZ/V5-His (Invitrogen) by deleting the OpIE2 (*Orgyia pseudotsugata* multicapsid nucleopolyhedrovirus *ie2*) promoter located in front of the multiple cloning sites. Next, part (~2 kbp) of the WSSV IE1 promoter fragment upstream of the ATG was amplified from the WSSV

\* Corresponding author. Mailing address: Institute of Zoology, National Taiwan University, Taipei 106, Taiwan. Phone: 886-2-33662453. Fax: 886-2-23638179. E-mail for Chu-Fang Lo: gracelow@ntu.edu.tw. E-mail for Guang-Hsiung Kou: ghkou@ntu.edu.tw.

<sup>∇</sup> Published ahead of print on 3 September 2008.

TABLE 1. Primers used for construction of luciferase reporter and effector plasmids

Plasmid	Primer(s)	Primer sequence (5'-3') <sup>a</sup>
pWSSV-IE1 <sub>1-224</sub> -V5-His	IE1-F IE1-R	TCCCCGCGGATGGCCTTTAATTTTGAAGAC TCCCCGCGGTACAAAGAATCCAGAAATCTCA
pWSSV-GAL4-IE1 <sub>1-224</sub> -V5-His	IE1-F/IE1-R	
p35 <sub>BAS</sub> -Luc	AcMNPV-p35-F1 AcMNPV-p35-R1	CCGCTCGAGTGGCGACGGATTTTATATACA CCCAAGCTTTTGGCAATGGTAAAGCTCAAAA CGGGGTACCGATCGGAGTACTGTCTCCG CCGCTCGAGCAAGCTAATTCGGGGGATC TCCCCGCGGGAGACGCCTTTCATCACCTC TCCCCGCGGTGCCAAGCAGTTGTCTTGAC TCCCCGCGGCCATTTTCATGGCTAGCGAAGT TCCCCGCGGAAACATTGGGTTTGATGCATT TCCCCGCGGAACAGTGGTTCCCATGTCAAG TCCCCGCGGGCATTATTCCTTCAAGAGTTT TCCCCGCGGTGGATGGCTAGGGATGTGACT TCCCCGCGGTACGGCAAGGAAAGTGTGG TCCCCGCGGTGCCAAGCAGTTTGTCTTGAC TCCCCGCGGGGCCAACACACAGACCTTAC TCCCCGCGGATCATATTCTTTGAAAGTCT TCCCCGCGGTCTGGTATTGAGGTGATGAAG TCCCCGCGGTGCTTCAAAAATCCACACTT TCCCCGCGGGAGCCAGAAATACACATAGC TCCCCGCGGGAGATTCTCCATATCTTCTGC
G5p35 <sub>BAS</sub> -Luc	GAL4bs-F GAL4bs-R	
pWSSV-GAL4-IE1 <sub>1-49</sub> -V5-His	IE1-F (see above)/IE1-49-R	
pWSSV-GAL4-IE1 <sub>1-92</sub> -V5-His	IE1-F (see above)/IE1-92-R	
pWSSV-GAL4-IE1 <sub>1-137</sub> -V5-His	IE1-F (see above)/IE1-137-R	
pWSSV-GAL4-IE1 <sub>1-186</sub> -V5-His	IE1-F (see above)/IE1-186-R	
pWSSV-GAL4-IE1 <sub>81-224</sub> -V5-His	IE1-81-F/IE1-R (see above)	
pWSSV-GAL4-IE1 <sub>92-224</sub> -V5-His	IE1-92-F/IE1-R (see above)	
pWSSV-GAL4-IE1 <sub>137-224</sub> -V5-His	IE1-137-F/IE1-R (see above)	
pWSSV-GAL4-IE1 <sub>50-92</sub> -V5-His	IE1-50-F IE1-92-R	
pWSSV-GAL4-IE1 <sub>20-92</sub> -V5-His	IE1-20-F/IE1-92-R (see above)	
pWSSV-GAL4-IE1 <sub>30-92</sub> -V5-His	IE1-30-F/IE1-92-R (see above)	
pWSSV-GAL4-IE1 <sub>40-92</sub> -V5-His	IE1-40-F/IE1-92-R (see above)	
pWSSV-GAL4-IE1 <sub>1-60</sub> -V5-His	IE1-F (see above)/IE1-60-R	
pWSSV-GAL4-IE1 <sub>1-70</sub> -V5-His	IE1-F (see above)/IE1-70-R	
pWSSV-GAL4-IE1 <sub>1-80</sub> -V5-His	IE1-F (see above)/IE1-80-R	

<sup>a</sup> Restriction enzyme cutting sites are underlined.

genomic DNA (using the primers CGGAATTCGATGATGGTATGTTTC TAGG and CCGCTCGAGCTTGAGTGGAGAGAGAGAGC [underlined sequences represent the restriction enzyme recognition sites]) and cloned into pIZΔIE/V5-His. The resulting plasmid was designated pWSSV-V5-His and was used to express the full-length *ie1* coding region, the GAL4 DBD (29), and various fusion proteins consisting of the GAL4 DBD plus downstream, in-frame insertions of different regions of the WSSV *ie1* coding sequence (see Table 1 for the *ie1* primers). To construct the GAL4 DBD gene plasmid (pWSSV-GAL4-V5-His), the gene sequence encoding GAL4 DBD amino acids (aa) 1 to 147 was amplified by PCR from yeast genomic DNA (using the primers 5'-GCTCTAGAATGAAGCTACTGTCTTCTATC-3' and 5'-TCCCCGCGGCGATACAGTCAACTGTCTTTG-3') and then cloned into the XbaI/SacII-digested pWSSV-V5-His plasmid. One of the fusion protein plasmids, pWSSV-GAL4-IE1<sub>1-80</sub>-V5-His, contained the wild-type IE1 sequence spanning aa 1 to 80, and this plasmid was used as a template to produce a range of N-terminal mutants. Site-directed mutations of the acidic residues of the amino terminus of IE1 were generated by using rolling-circle PCR (20) to replace the acidic residues with alanine. To confirm that only the acidic amino acids were involved in transactivation, alanine was also used to replace two randomly chosen nonacidic residues (G20A and G41A mutations). Mutations were verified for all plasmids by DNA sequencing analysis. The specifically designed mutagenic primers used to generate the IE1 TAD mutants are listed in Table 2.

(ii) **Luciferase reporters.** The reporter plasmid p35<sub>BAS</sub>-Luc, which contained the firefly luciferase reporter gene, was constructed by PCR cloning of the *Autographa californica* multicapsid nucleopolyhedrovirus (AcMNPV) p35 basal promoter into the pGL3-Basic vector (Promega), using the primer pair AcMNPV-p35-F1 and AcMNPV-p35-R1 (Table 1). The other reporter plasmid, G5p35<sub>BAS</sub>-Luc, contained five copies of the GAL4 DNA binding site upstream of the AcMNPV p35 basal promoter, and it was constructed by amplifying five copies of the GAL4 DNA binding site from pG5SEAP (Clontech), using primers GAL4bs-F and GAL4bs-R (Table 1), and then cloning them into p35<sub>BAS</sub>-Luc vector KpnI and XhoI sites.

(iii) **Glutathione S-transferase-IE1 (GST-IE1) and GST-VP36B.** The plasmids pGST-IE1<sub>1-224</sub> and pGST-IE1<sub>81-224</sub> were generated by cloning PCR-amplified WSSV *ie1* coding region fragments flanked by EcoRI and XhoI restriction sites into the corresponding sites of predigested pGEX-5X-1 vector (Amersham Pharmacia Biotech). pGST-IE1<sub>81-224</sub> C2-H2mut was constructed by rolling-circle PCR as described above, using pGST-IE1<sub>81-224</sub> as the template. The plasmid pGST-VP36B was constructed by cloning the WSSV structural protein VP36B into the pGEX-5X-1 vector, using primers VP36B-F and VP36B-R. Primer sequences are listed in Table 3.

(iv) **IE1 expression plasmids.** PCR cloning was used to insert the WSSV *ie1* coding region into the vectors pDHsp/V5-His and pDHsp/FLAG-His, which both contain the heat-inducible *Drosophila* heat shock protein 70 promoter (28). The resulting plasmids, pDHsp/IE1-V5-His and pDHsp/IE1-FLAG-His, expressed the V5 and FLAG tag fusion proteins, respectively. Another IE1 expression plasmid, pcDNA3/IE1, was constructed by PCR cloning the WSSV *ie1* coding region into the commercialized vector pcDNA3 (Invitrogen). Primer sequences are listed in Table 3.

**Transient transfections and dual-luciferase reporter assay.** Transfections of Sf9 insect cells were performed using the Cellfectin reagent (Invitrogen). Briefly, the Sf9 insect cells were seeded onto a 24-well plate (1 × 10<sup>5</sup> cells/well) and grown in Sf-900 II serum-free medium (Invitrogen) overnight at 27°C. Cells were

TABLE 2. Sequences of mutated oligonucleotides used to generate point mutations in the WSSV IE1 transactivation domain

Plasmid	Primer sequence (5'-3') <sup>a</sup>
pWSSV-GAL4-IE1 <sub>1-80</sub> .....	TTTGCCAATATGGACTTGAC (E6A/D7A) GAGATTTGTAGAGGCTGCAAA
pWSSV-GAL4-IE1 <sub>1-80</sub> .....	TTTGCCAATATGGCCTTGAC (D16A) GAGATTTGTAGACTTCTCAAA
pWSSV-GAL4-IE1 <sub>1-80</sub> .....	CGCCCAATATCATATTCCTT (D24A) GGTAGGGGCTGTTGTTGTGCC
pWSSV-GAL4-IE1 <sub>1-80</sub> .....	GGGAGTAGACTTGCAAAGAA (E34A/E43A) AACTCTGGTATTGCGGTGATG
pWSSV-GAL4-IE1 <sub>1-80</sub> .....	GGGAATTTGCAGCAAGTGGA (E59A) ACACCTTTCCTTGCCGTACGAG
pWSSV-GAL4-IE1 <sub>1-80</sub> .....	TGGCTCGCAGCTAATGCAGAA (E71A/D72A) GAAATACGACATAGCACCTC
pWSSV-GAL4-IE1 <sub>1-80</sub> .....	AATGCAGCAGCTATGGAGAATC (E75A/D76A) ATCTTCGAGCCAGAAATACGA
pWSSV-GAL4-IE1 <sub>1-80</sub> .....	GCAGAAGATATGGCGAATCTC (E78A) ATTATCTTCGAGCCAGAAATA
pWSSV-GAL4-IE1 <sub>1-80</sub> .....	ACGGCTGCCAACAACAGAC (G20A) CAAGTCCATATTGGCAAAGAG
pWSSV-GAL4-IE1 <sub>1-80</sub> .....	AACTCTGCTATTGAGGTGATG (G41A) GGGAGTAGACTTTCAAAGAA

<sup>a</sup> The underlined nucleotides show the positions of the mutations. Plasmids with three or more mutations were constructed by nested PCRs using appropriate combinations of the primer sets.

TABLE 3. Primers used for construction of GST-IE1 fusion proteins and IE1 expression plasmids

Plasmid	Primer	Primer sequence (5'-3') <sup>a</sup>
pGST-IE1 <sub>1-224</sub>	IE1-1-F IE1-224-R	<u>CGGAATTCATGGCCTTTAATTTTGAAGACTC</u> <u>CCGCTCGAGTTATACAAAGAATCCAGAAATC</u>
pGST-VP36B	VP36B-F VP36B-R	<u>GCATGAATTCATGGCGGTAAACTTGGATAATG</u> <u>GCAGCTCGAGTTATGTCCAACAATTTAAAAAG</u>
pGST-IE1 <sub>81-224</sub>	IE1-81-F/IE1-224-R (see above)	<u>CGGAATTC</u> CAACAGTGGTCCCATGTCAAG
pGST-IE1 <sub>81-224</sub> C2-H2mut	IE1-C2-mut-F IE1-C2-mut-R IE1-H2-mut-F IE1-H2-mut-R	<u>TGTAGGGCCAAGTACCCAGGC</u> <u>CGCATTAGCTACAGAAAACAT</u> <u>GGTGCTTCTGATTTGACATGT</u> <u>CACTCCAGCGCCTTCAATAAC</u>
pDHsp/IE1-V5-His	IE1-HindIII-F IE1-SacII-R	<u>CCCAAGCTTCTCAAGATGGCCTTTAATTTTG</u> <u>TCCC CGCGGTACAAAGAATCCAGAAATCTCA</u>
pDHsp/IE1-FLAG-His	IE1-HindIII-F (see above)/IE1-SacII-R (see above)	
pCDNA3/IE1	IE1-HindIII-F (see above)/IE1-XhoI-R	<u>CGCTCGAGTTATACAAAGAATCCAGAAAT</u>
pET-28b(+)/IE1	IE1-NdeI-F/IE1-XhoI-R (see above)	<u>CCCATATGGCCTTTAATTTTGAAGAC</u>

<sup>a</sup> Restriction enzyme cutting sites or mutated sites are underlined.

cotransfected with 300 ng of the reporter plasmid containing the firefly luciferase gene, 500 ng of one of the different effector plasmids or the empty vector, and 100 ng of the *Renilla* luciferase gene plasmid, phRL/AcMNPVie1 (30). The phRL/AcMNPVie1 plasmid contains the AcMNPV *ie1* promoter to drive the expression of the *Renilla* luciferase gene and was used to monitor and normalize transfection efficiency. Cells were collected at 48 h posttransfection, and the cell lysates were prepared according to the Promega instruction manual for the dual-luciferase assay system. Luciferase activities were measured with a luminometer (Labsystems). Firefly luciferase activity values were then normalized against the activities of the *Renilla* luciferase to correct for transfection efficiency, and data were expressed as relative luciferase activities. Luciferase activities were determined for triplicate transfections in two independent experiments, and the means and standard deviations (SD) were calculated. For the point mutation assays, statistically significant differences from the wild-type TAD expression plasmid were identified using paired Student's *t* test, with significance set at *P* values of <0.01.

**Cell extracts and Western blot analysis.** Total cell lysates were prepared by directly adding 2× sodium dodecyl sulfate-polyacrylamide gel electrophoresis (SDS-PAGE) sample buffer (100 mM Tris-HCl [pH 6.8], 200 mM dithiothreitol [DTT], 4% SDS, 0.2% bromophenol blue, 20% glycerol) to cell pellets and then boiling the samples for 10 min. The samples were separated in 15% polyacrylamide gels, transferred to a polyvinylidene difluoride membrane (MSI), incubated with either anti-V5 antibody (Sigma) or anti-β-actin antibody (Chemicon), and then detected with a secondary peroxidase-conjugated antibody. Detected proteins were visualized using an ECL (Perkin-Elmer) detection system.

**Expression and purification of GST, GST-VP36B, GST-IE1<sub>1-224</sub>, and GST-IE1 deletion mutants.** GST fusion proteins were expressed and purified according to the manufacturer's manual. After overnight culture of the GST plasmids in transformed *Escherichia coli* BL21 Codon Plus cells (Stratagene), the cultures were diluted 1:200 (vol/vol) in Luria-Bertani (LB) medium containing 50 μg/ml of ampicillin and then incubated for another 3 h at 37°C. Expression of the fusion proteins was induced by the addition of IPTG (isopropyl-β-D-thiogalactopyranoside) to a final concentration of 1 mM, and the cultures were grown for a further 24 h at 15°C. The soluble GST fusion proteins were resuspended in lysis buffer (50 mM Tris-HCl [pH 8.0], 300 mM NaCl, 1 mM DTT, and 1 mM EDTA) and purified by affinity chromatography with an FF 16/10 GST column (Amersham Biosciences). The fusion proteins were eluted from the beads with 50 mM Tris-HCl (pH 8.0), 300 mM NaCl, 1 mM DTT, 1 mM EDTA, and 10 mM reduced glutathione, and then the purified proteins were condensed with an Amicon Ultra-30 column (Millipore). To obtain the IE1<sub>1-224</sub> protein, the GST was removed from the GST-IE1<sub>1-224</sub> fusion protein by digestion with factor Xa (10 units of protease/1 mg GST fusion protein; Amersham Biosciences) in 1× phosphate-buffered saline (PBS) containing 1 mM DTT at 22°C for 16 h. The digested GST was removed with a GST column. Purity of the samples was assessed by SDS-PAGE, and the protein concentration was determined using a Bio-Rad protein assay kit.

**DNA binding assay (EMSA).** EMSA was performed as described previously (49), with some modifications. Single-stranded oligonucleotides containing a 25-nucleotide random core sequence flanked on each side by 27 nucleotides [5'-GTCGCTCGAGCGGTATGACGAGATCTA(N)<sub>25</sub>TAGATCTGCGTCAC TAGTCTAGACTAG-3' (where N can be any of the four deoxyribonucleotides)]

were synthesized (9). A double-stranded [ $\alpha$ -<sup>32</sup>P]dCTP-labeled oligonucleotide library was generated by PCR using the forward primer 5'-GTCGCTCGAGCGGTATGACG-3' and the reverse primer 5'-CTAGTCTAGACTAGTACGCG-3'. Binding reactions were carried out for 30 min at room temperature in 15-μl reaction mixtures that contained different concentrations of purified recombinant proteins with 10 mM HEPES (pH 7.9), 1 mM DTT, 5 mM MgCl<sub>2</sub>, 0.5 mM ZnCl<sub>2</sub>, 60 mM KCl, 0.05% NP-40, 200 ng poly(dI-dC), 10% glycerol, and 50 μg/ml bovine serum albumin. The DNA-protein complexes were resolved in 7.5% polyacrylamide gels in 0.5× Tris-glycine buffer (12.5 mM Tris and 100 mM glycine). The gels were dried and visualized by autoradiography. Some EMSA reactions were run with no ZnCl<sub>2</sub> in the binding buffer.

**In vitro protein synthesis and GST pull-down assay.** Coupled in vitro transcription-translation reactions were conducted using a TNT kit in accordance with the manufacturer's protocol (Promega). One microgram of plasmid pCDNA3/IE1 DNA and 2 μl of [<sup>35</sup>S]methionine (1,000 Ci/mmol; 10 mCi/ml) were added to the TNT mixture (50-μl total volume), and reactions were carried out at 30°C for 90 min. To ensure that there was no contamination by nucleic acids, the purified proteins GST and GST-IE1<sub>1-224</sub> and the TNT product [<sup>35</sup>S]methionine-labeled IE1 were all pretreated with nucleases (1 U DNase I [Invitrogen] and 0.5 μg RNase [Sigma]) for 1 h at 25°C in 50 mM Tris-HCl, pH 8, 5 mM MgCl<sub>2</sub>, 2.5 mM CaCl<sub>2</sub>, 100 mM NaCl, 5% glycerol, and 1 mM DTT. Subsequently, equal amounts of the TNT product were incubated with GST-IE1<sub>1-224</sub> (10 μg) or GST (10 μg) bound to glutathione-Sepharose beads in 150 μl NETN buffer (20 mM Tris-HCl [pH 8.0], 100 mM NaCl, 1 mM EDTA, 0.5% NP-40, and a cocktail tablet of protease inhibitors [Roche]) in the presence of ethidium bromide (100 μg/ml) at 4°C for 3 h. After three 10-min washes with NETN buffer, the proteins that bound to the beads were resolved by 15% SDS-PAGE, and the gel was dried and exposed to Kodak Biomax MS film.

**Coimmunoprecipitation.** Sf9 cells were seeded on six-well plates (8 × 10<sup>5</sup> cells/well) and cotransfected with 2 μg pDHsp/IE1-V5-His and 2 μg pDHsp/IE1-FLAG-His expression plasmid, using Cellfectin reagent. After transfection for 16 to 18 h, the cells were heat shocked in a 42°C water bath for 30 min and then returned to 27°C. Six hours after being heat shocked, the cells were washed with PBS and lysed in 100 μl of NP-40 lysis buffer (50 mM Tris-HCl, pH 8.0, 150 mM NaCl, 1% NP-40) supplemented with a protease inhibitor cocktail tablet. The lysis procedure was carried out on ice for 10 min with occasional shaking. The lysate was centrifuged at 12,000 × *g* for 5 min, and an aliquot of the supernatant (10 μl) was reserved for immunoblot analysis to confirm the expression of the transfected gene. The remaining supernatant (90 μl) was then incubated with 15 μl of anti-FLAG M2 affinity gel (Sigma) at 4°C overnight with rotation. The gel was then washed five times in 150 μl of NP-40 lysis buffer. Aliquots of the total cell lysates and immunoprecipitates were separated by 15% SDS-PAGE and transferred to a polyvinylidene difluoride membrane. V5-tagged IE1 fusion proteins were detected with rabbit anti-V5 antibody (Sigma) and goat anti-rabbit immunoglobulin G-horse radish peroxidase conjugate (Sigma). FLAG-tagged IE1 was detected with mouse anti-FLAG monoclonal antibody (Sigma) and goat anti-mouse immunoglobulin G-horse radish peroxidase conjugate (Sigma).

**Gel filtration.** To evaluate the native molecular size of IE1, purified IE1<sub>1-224</sub> was analyzed using a Superdex 200-pg gel filtration column (Amersham Biosciences) (using buffer comprised of 500 mM NaCl, 1 mM DTT, 1 mM EDTA,

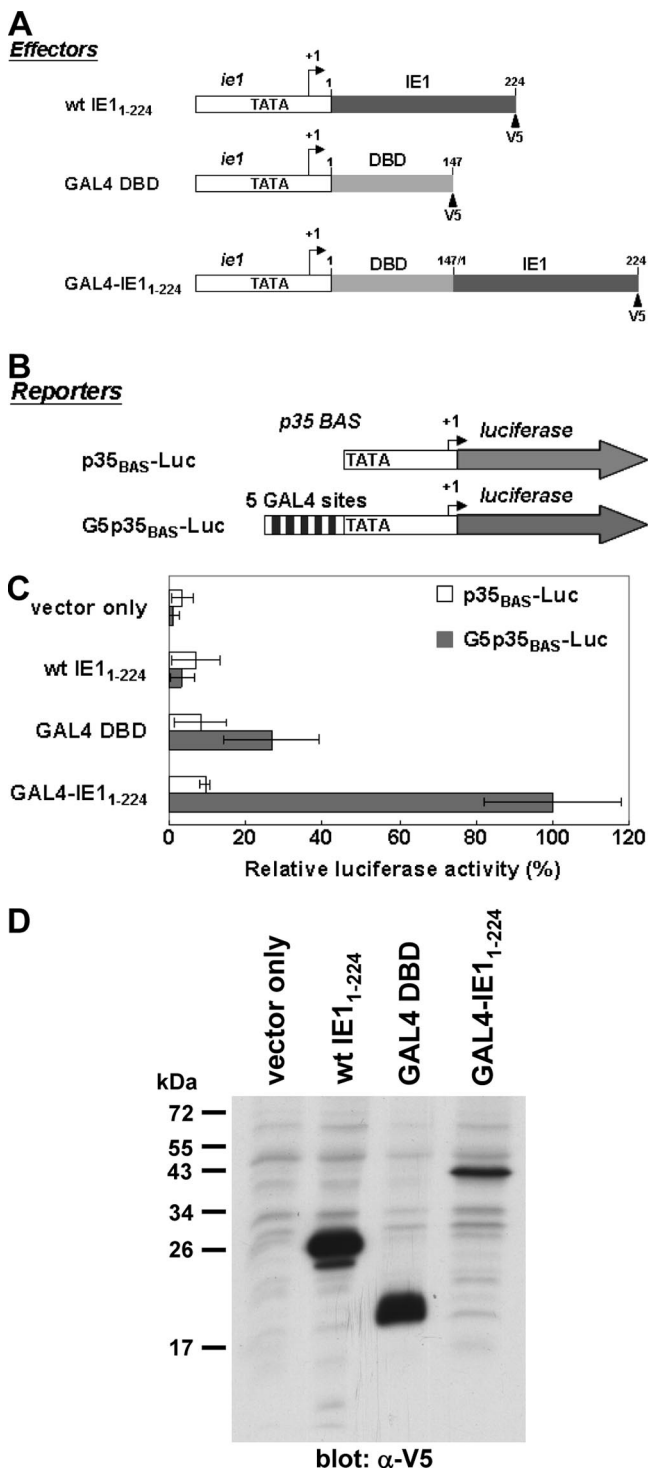


FIG. 1. GAL4-dependent IE1 transactivation. (A) Schematic representation of the three effector plasmids. For wild-type (wt) IE1<sub>1-224</sub>, amino acids 1 to 224 from IE1 (dark gray bar) were placed under the control of the WSSV *ie1* promoter. GAL4 DBD had aa 1 to 147 of the GAL4 DBD (gray bar). For the hybrid GAL4-IE1<sub>1-224</sub>, both sequences were fused as shown. The V5 epitope (arrowhead) was inserted after DBD residue 147 or IE1 residue 224. (B) The reporter plasmid p35<sub>BAS</sub>-Luc contains the baculovirus *p35* basal (BAS) promoter (TATA box and RNA start site) linked to the firefly luciferase gene (dark gray arrow). G5p35<sub>BAS</sub>-Luc is identical to p35<sub>BAS</sub>-Luc except for the presence of five GAL4 binding sites (solid boxes) upstream of the

and 20 mM sodium acetate, pH 5.5). Gel filtration standard proteins (bovine serum albumin [67 kDa], ovalbumin [43 kDa], chymotrypsinogen A [25 kDa], and RNase A [13.7 kDa]) were used to calibrate the column. For each protein, the logarithm of molecular mass was plotted against  $K_{av}$ , which was calculated as follows:  $K_{av} = (V_e - V_o)/(V_t - V_o)$ , where  $V_e$  is the elution volume,  $V_o$  is the column void volume using blue dextran 2000, and  $V_t$  is the total column bed volume (120 ml for Superdex 200-pg gel filtration column).

**WSSV IE1 antibody preparation.** A PCR fragment representing the coding region of *ie1* was amplified using the IE1-NdeI-F/IE1-XhoI-R primer set (Table 3), digested with restriction enzymes, and cloned into pET-28b(+) (Novagen). The resulting pET clone was transformed into BL21 cells. For protein expression and purification, the cells were grown overnight at 37°C in LB medium supplemented with 50 µg of kanamycin/ml and 34 µg of chloramphenicol/ml. The cells were inoculated into new medium at a ratio of 1:50 and grown at 37°C for 2 to 2.5 h. Expression was induced by the addition of 1 mM IPTG, and incubation was continued for another 1.5 to 3 h. The induced bacteria were spun down at 4°C, suspended in ice-cold PBS containing 10% glycerol and a protease inhibitor cocktail tablet, and then sonicated for 3 min on ice. The insoluble debris was collected by centrifugation, suspended in PBS containing 1.5% sodium lauryl sarcosine, and solubilized by shaking at room temperature for 1 h. The supernatant was clarified by centrifugation and mixed with Ni-nitrilotriacetic acid-agarose beads (Qiagen) on a rotating wheel at 4°C for 16 h or overnight. The beads were then washed several times with ice-cold wash buffer (1 M NaCl, 10 mM Tris-HCl, pH 7.5) to remove unbound material. The fusion proteins were eluted directly from the beads with SDS sample buffer and then subjected to SDS-PAGE analysis. The protein bands containing the fusion proteins were sliced from the gel, minced, mixed with Freund's adjuvant, and used for antibody production.

**Glutaraldehyde cross-linking of proteins.** For protein polymerization assays, Sf9 cells were transfected with pDHsp/IE1-V5-His plasmid DNA and heat shocked as described above. The transfected cells were then washed with PBS, lysed in a hypotonic buffer (10 mM Tris-HCl [pH 7.5], 10 mM KCl, and 5 mM MgCl<sub>2</sub>), and incubated on ice for 20 min. The swollen cells were passed through a 25-gauge needle 20 times to disrupt the cells. After centrifugation at 1,000 × g, the supernatant was incubated with glutaraldehyde (Sigma) at a final concentration of 0.01% at room temperature for various times. The reactions were stopped by the addition of an equal volume of 2× SDS sample buffer, and the samples were subjected to Western blotting using IE1 polyclonal antibody.

**RESULTS**

**WSSV IE1 contains TADs.** As an initial indication of whether the WSSV IE1 gene product contains a transcriptional activation domain, the IE1 gene was fused to sequences encoding the 147-aa DBD of the yeast transcriptional activator GAL4 (Fig. 1A). GAL4-IE1<sub>1-224</sub> transactivation was monitored in transient expression assays in which Sf9 cells were transfected with a reporter plasmid that contained the luciferase gene under the control of the basal promoter of the AcMNPV *p35* gene, with (G5p35<sub>BAS</sub>-Luc) or without (p35<sub>BAS</sub>-Luc) GAL4 DNA binding sites (Fig. 1B). The results showed that GAL4-IE1<sub>1-224</sub> transactivation of the AcMNPV *p35* basal promoter was about 10 times greater when the reporter plas-

TATA element. (C) Transactivation by GAL4-IE1<sub>1-224</sub>. Sf9 cells were cotransfected with 300 ng of the indicated reporter plasmid, 500 ng of one of the different effector plasmids or empty vector, and 100 ng of the *Renilla* luciferase gene plasmid, phRL/AcMNPVie1, to correct for transactivation efficiency. Relative luciferase activity was normalized to that of G5p35<sub>BAS</sub>-Luc with GAL4-IE1<sub>1-224</sub>, which was arbitrarily set to 100%. Data show the means of six repetitions, and error bars show the SD. (D) Western blot analysis was used to confirm the expression of chimeric GAL4-IE1<sub>1-224</sub>, GAL4 DBD, and IE1<sub>1-224</sub> proteins. Protein extracts corresponding to approximately 1 × 10<sup>5</sup> cells/lane were separated by SDS-PAGE and examined by Western blot analysis with an anti-V5 antiserum.

mid included the five GAL4 binding sites (Fig. 1C). In contrast, the presence of the GAL4 DNA binding sites had no effect on the low transactivation activity exhibited by the wild-type IE1<sub>1-224</sub> construct, while the GAL4 DBD control also showed only low levels of transactivation (Fig. 1C). Expression of the various constructs was confirmed by Western blotting (Fig. 1D). We concluded that WSSV IE1 contains at least one domain that functions as a transcriptional activator. This conclusion was further supported by yeast two-hybrid experiments showing that WSSV IE1 is a strong autoactivator (data not shown).

**Mapping of the WSSV IE1 TAD.** In order to determine the essential domains for transactivation, three series of deletion mutants of WSSV IE1 were generated and constructed as fusion proteins with the GAL4 DBD at the N terminus (Fig. 2A, B, and C). Additional V5 tags were attached to the C termini of these fusion proteins for Western blot analysis (Fig. 2D). The various constructs encoding the IE1 deletion mutants were transfected into Sf9 cells together with the GAL4-responsive reporter plasmid G5p35<sub>BAS</sub>-Luc. Surprisingly, coarse mapping (Fig. 2A) showed that the transactivation activity of most of the IE1 mutants was almost completely abolished, except for that of GAL4-IE1<sub>1-92</sub>, which exhibited an activity that was 2 times higher than that of the full-length IE1 fusion protein and 5.4 times higher than that of the GAL4 DBD construct. These initial results suggested that WSSV IE1 residues 1 to 92 function as a TAD, that residues 50 to 92 may be critical for this function (compare GAL4-IE1<sub>1-49</sub> to GAL4-IE1<sub>1-92</sub>), and that residues 93 to 137 may inhibit this transactivation activity (compare GAL4-IE1<sub>1-92</sub> to GAL4-IE1<sub>1-137</sub>). Next, the series of N-terminal and C-terminal truncation constructs, shown in Fig. 2B and C, respectively, were designed to more finely delineate the boundaries of the N-terminal activation domain. Transfection with these series showed that residues 1 to 80 exhibited an even stronger transactivation activity than residues 1 to 92 did (Fig. 2C), which is consistent with the results for GAL4-IE1<sub>81-224</sub> versus GAL4-IE1<sub>92-224</sub> (Fig. 2A). These results suggest that the minimal IE1 TAD may be located within aa 1 to 80. Two additional potential inhibitory domains were also identified. The results of deletions made in the region of aa 1 to 49 suggested that amino acid residues 41 to 49 might act as an inhibitory domain (Fig. 2B, compare GAL4-IE1<sub>50-92</sub> to GAL4-IE1<sub>20-92</sub>, GAL4-IE1<sub>30-92</sub>, and GAL4-IE1<sub>40-92</sub>). The other possible inhibitory domain was identified at residues 81 to 92 (Fig. 2C, compare GAL4-IE1<sub>1-92</sub> to GAL4-IE1<sub>1-80</sub>), although we note that the different activation levels might have been due, at least in part, to the larger quantity of expressed GAL4-IE1<sub>1-80</sub> fusion protein. The Western blots in Fig. 2D confirmed that all of these constructs were successfully expressed. Note that every deletion mutant had a higher expression level than that of the wild-type IE1 fusion protein (compare Fig. 2D to Fig. 1D). These higher expression levels were probably due to the shorter lengths of the transcripts and encoded proteins, which would lead to increased transcriptional and translational efficiencies.

**Negatively charged amino acids are important for IE1 transactivation activity.** Sequence analysis shows that there are 12 acidic amino acids and 6 basic residues in the IE1 minimal TAD (aa 1 to 80), giving the TAD a net negative charge of -6 and a pI of 4.3. Since most TADs can be classified as either acidic activators (46), glutamine-rich activators (11), aromatic

and hydrophobic activators (44), or proline-rich activators (37), the acidity of the WSSV IE1 TAD suggested that it might fall within the acidic class of activation domains. We investigated this possibility by constructing mutants (Table 2) in which alanine (A) was used to replace the wild-type aspartate (D), glutamate (E), or glycine (G) residues. GAL4 transactivation assays showed that almost all of these alanine substitutions significantly reduced G5p35<sub>BAS</sub>-Luc activation ( $P < 0.01$ ). Replacement of increasing numbers of acidic residues led to a further decrease in transactivation activity (Fig. 3A), while substitutions of nonacidic residues (G20A and G41A) (Fig. 3A) had no significant effect on transactivation. We therefore concluded that the negatively charged residues are critical for WSSV IE1 transactivation activity. An immunoblot analysis of the mutated IE1 proteins after a typical transfection showed that most of the alanine substitution mutants produced proteins at levels close to that of the wild-type construct (Fig. 3B). Only the E71A/D72A mutant exhibited a very low level of protein expression. This may have been due to instability and rapid degradation of the expressed protein, which might in turn explain why this protein exhibited the lowest transactivation activity in Fig. 3B. Meanwhile, the results for all other mutants indicate that in the case of IE1, as with other virus immediate-early proteins, specific acidic amino acids are particularly critical to transcriptional function (6, 15).

**DNA binding activity of WSSV IE1.** The DNA binding activity of WSSV IE1 was investigated by gel mobility shift assays using a 79-bp double-stranded DNA oligonucleotide containing a central 25-bp randomized sequence. GST-tagged versions of IE1 and VP36B (a WSSV structural protein which served as a negative control) were expressed in *E. coli* to produce either GST-IE1<sub>1-224</sub>, GST-VP36B, or IE1<sub>1-224</sub> alone. These soluble, well-expressed proteins were then purified with glutathione-Sepharose beads (Fig. 4A). The entire purification process was conducted in the presence of EDTA to ensure that the expressed proteins were free of Zn<sup>2+</sup> contamination. Purified IE1<sub>1-224</sub> and GST-IE1<sub>1-224</sub> proteins both retarded the migration of the oligonucleotide and formed major discrete bands by 7.5% native PAGE (Fig. 4B, lanes 4 to 6 and 7 to 9, respectively). Furthermore, the intensities of these bands increased with increasing amounts of purified protein. In contrast, no complex was formed with the GST or with the purified WSSV structural protein control GST-VP36B (Fig. 4B, lanes 1 to 3 and 11). The last three lanes in Fig. 4B show that Zn<sup>2+</sup> is not required for the DNA binding activity of IE1<sub>1-224</sub>. These preliminary data suggested that even though the *ie1* coding region contains a Cys<sub>2</sub>/His<sub>2</sub>-type zinc finger motif (X<sub>3</sub>-Cys-X<sub>3-4</sub>-Cys-X<sub>12</sub>-His-X<sub>3-4</sub>-His-X<sub>4</sub>) (31), WSSV IE1 may not in fact be a zinc finger protein. This was further investigated in the following experiments.

**The WSSV IE1 C-terminal region is required for DNA binding.** Since DBDs and TADs usually do not overlap, we hypothesized that the DBD of IE1 was located in the C-terminal region. To test this hypothesis, we expressed and purified two GST-IE1 proteins: GST-IE1<sub>81-224</sub> was a deletion without the N-terminal TAD, and GST-IE1<sub>81-224C2-H2mut</sub> was identical except for a mutated zinc finger motif (Fig. 5A). An SDS-PAGE gel of these two fusion proteins is shown in Fig. 5B. The lower band, at ~26 kDa, was confirmed by Western blot analysis to be nonfused GST (data not shown). The EMSA showed that

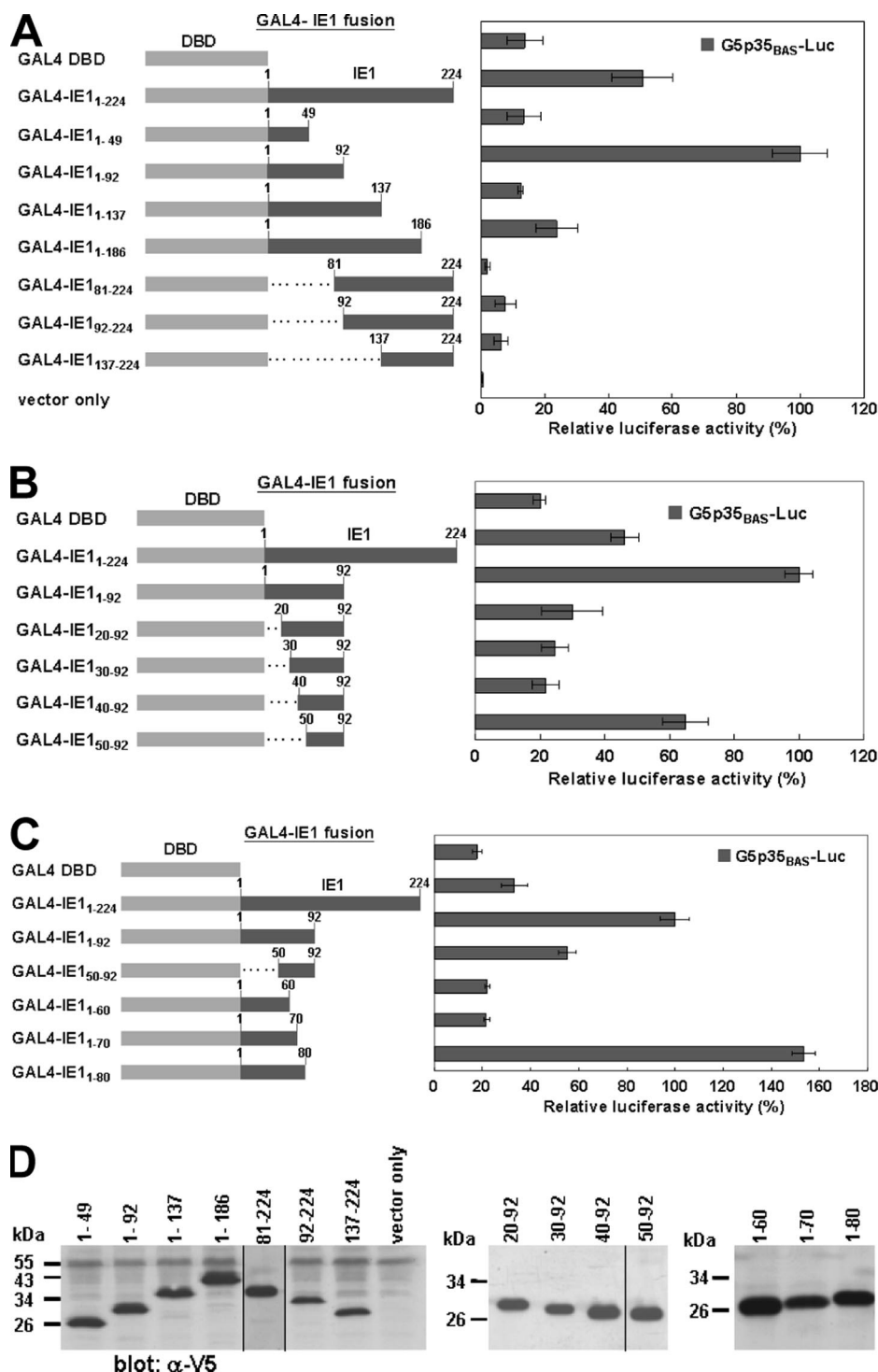


FIG. 2. Identification of IE1 TAD. (A to C) Three series of deletion assays to identify the location of the IE1 TAD. The GAL4-IE1 fusion proteins were constructed by joining the GAL4 DBD from amino acids 1 to 147 (gray bar) to the indicated segments of IE1 (dark gray bars). Sf9 cells were cotransfected with reporter plasmid G5p35<sub>BAS</sub>-Luc, the indicated GAL4-IE1 fusion plasmids, GAL4 DBD, or empty vector, and 100 ng of the *Renilla* luciferase gene plasmid, pHR1/AcmNPVie1, and then assayed for luciferase activity. Relative luciferase activities were normalized with respect to that of GAL4-IE1<sub>1-92</sub>, which was arbitrarily set to 100%. Data show the means of six repetitions, and error bars show the SD. (D) Western blot analysis of chimeric GAL4-IE1 proteins was performed as described in the legend to Fig. 1.

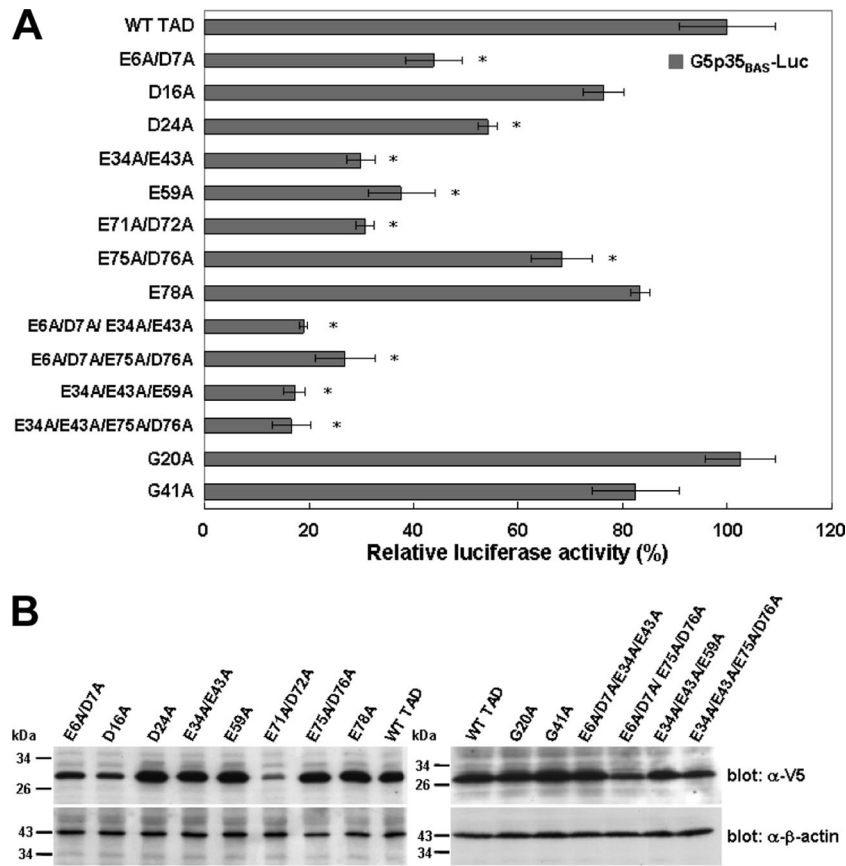


FIG. 3. Effects of substituting alanine (A) for the negatively charged acidic amino acids in the IE1 TAD. Labels indicate the original amino acid(s) (D, aspartate; E, glutamate; and G, glycine [control]) and its location relative to the N terminus of the IE1 coding region. (A) The reporter plasmid was cotransfected into Sf9 cells with effector plasmids expressing the IE1 wild-type TAD or the indicated point mutants and with the *Renilla* luciferase gene plasmid. Relative luciferase activities were normalized with respect to that of GAL4-IE1<sub>1-80</sub> (wild-type TAD), which was defined as 100%. Data show the means of six repetitions, and error bars show the SD. Activities that were significantly different from that of wild-type TAD are indicated with asterisks ( $P < 0.01$ ). (B) Western blot analysis of GAL-IE1 wild-type TAD and its substitution mutants was performed as described in the legend to Fig. 1. The lower panel shows the internal control: total proteins were probed using anti- $\beta$ -actin antibody.

when the TAD was deleted, IE1 was still able to bind DNA in either the presence or absence of  $Zn^{2+}$  (Fig. 5C, lanes 2 to 4 and 5 to 7). When the deletion's zinc finger domain was point mutated, DNA binding activity was not markedly affected in either the presence or absence of  $Zn^{2+}$  (Fig. 5C, lanes 8 to 10 and 11 to 13). The binding activity of the mutant was not affected by the presence of  $Zn^{2+}$  ions.

**IE1 has a strong affinity for self-interaction.** Many virus immediate-early proteins are in dimeric form when they bind to DNA (8, 16, 40, 57). We therefore performed an in vitro biochemical binding assay to determine whether IE1 can also self-interact directly. For this assay, the GST-IE1<sub>1-224</sub> fusion protein was bound to glutathione-Sepharose beads and incubated with in vitro-translated, [<sup>35</sup>S]methionine-labeled IE1. SDS-PAGE analysis showed that <sup>35</sup>S-labeled IE1 bound to the GST-IE1<sub>1-224</sub> fusion protein but not to GST, indicating that IE1 can interact directly with itself (Fig. 6A). We also studied the homotypic interaction between IE1 proteins by a coimmunoprecipitation assay using V5-tagged and FLAG-tagged versions of IE1 expressed in Sf9 insect cells. Complexes consisting of IE1-V5 plus IE1-FLAG were coimmunoprecipitated by anti-FLAG antiserum and detected by Western blotting using

anti-V5 antibody (Fig. 6B). Both sets of results indicated that IE1 can undergo specific self-interaction directly.

**IE1 protein forms a dimer.** Both gel filtration chromatography and chemical cross-linking were used to investigate the form of IE1 polymerization. Gel filtration chromatography using a Superdex 200-pg gel filtration column revealed that the major peak of purified IE1 eluted with an apparent molecular size of 46 kDa, as calculated from the logarithm of molecular size against the  $K_{av}$  values of protein standards that were fractionated in the same column (Fig. 6C, inset). In addition to the major elution fraction, some IE1 was also found in fractions where the 25-kDa chymotrypsinogen A appeared (Fig. 6C). Since IE1 is composed of 224 aa residues, with a molecular size of approximately 25 kDa, these results suggest that a portion of IE1 is in the monomeric state, most likely in dynamic equilibrium with the dimeric form. This finding suggested that IE1 exists mainly as a dimer in solution. For the cross-linking study, Sf9 cells were transfected with an expression plasmid that contained the full-length IE1 coding region under the control of the *Drosophila* heat shock protein 70 promoter. The cellular lysates were cross-linked with glutaraldehyde, and IE1 was detected by immunoblotting using anti-IE1 antibody. With in-

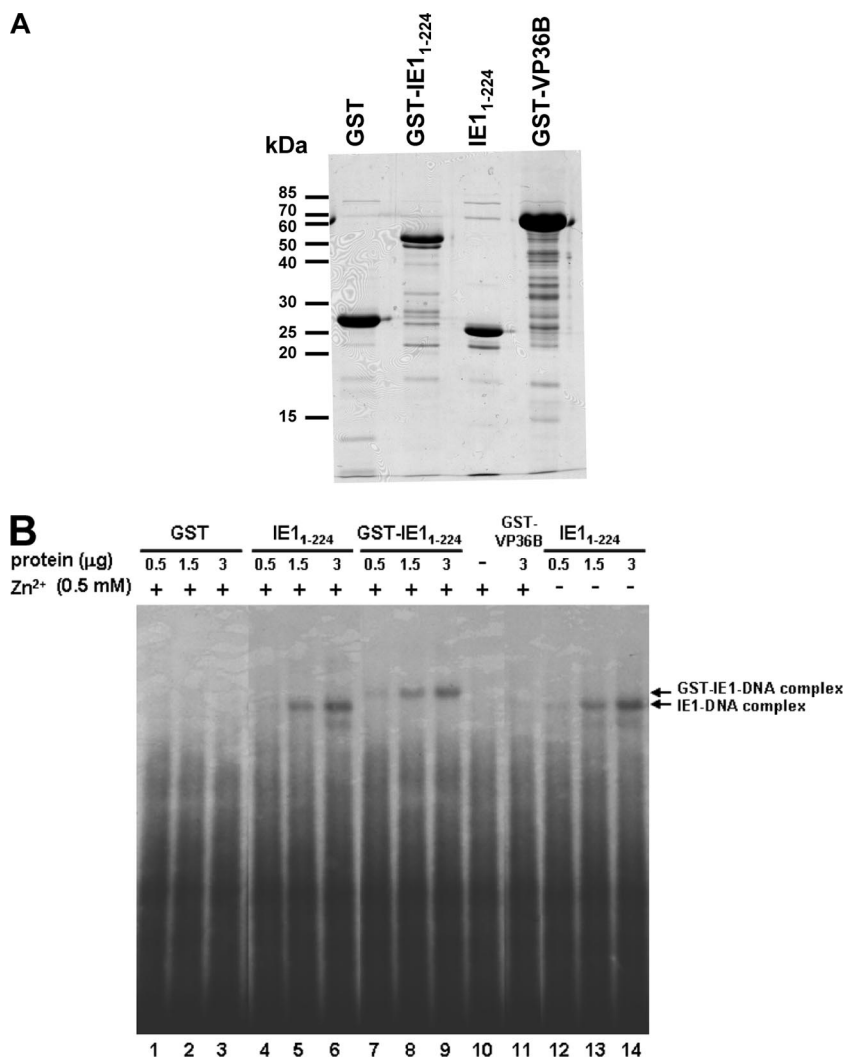


FIG. 4. DNA binding activity of IE1 and effect of zinc ions on DNA binding. (A) SDS-PAGE analysis of purified proteins used for EMSA. (B) EMSA was performed with a radiolabeled 79-bp DNA probe and 0.5 to 3  $\mu\text{g}$  of the indicated proteins. Lane 10 contained no protein and was used as a negative control. The bands containing the protein-DNA complexes are indicated.

creasing treatment time, there was a steady accumulation of dimeric (50 kDa) IE1 (Fig. 6D). Since IE1 was expressed at extremely high levels under these conditions, the amount of monomeric polypeptide (25 kDa) did not decrease significantly, even when there was extensive dimer formation.

## DISCUSSION

Our data suggest that the IE1 residues sufficient for transactivation are confined to the N terminus (Fig. 2). The N-terminal stretch of IE1 from residues 1 to 80 is highly acidic, with a net charge of  $-6$  and a theoretical pI of 4.3. Acid-rich transactivation regions are characteristic of acidic transactivators (26, 46), and to determine which amino acids are involved in mediating the activity of this domain, point mutations were introduced into the sequence. Our results (Fig. 3A) showed that the double mutations generally had a greater effect on activation than the single mutations did, that the triple and quadruple mutations had an even greater effect, and that the

glycine mutants were not significantly different from the wild-type TAD control. This is in broad agreement with previous mutational analyses of the activation domains of GAL4, GCN4, and the herpes simplex virus (HSV) transactivator VP16, all of which revealed a positive correlation between the number of acidic amino acids and the transcriptional ability of the acidic activation domains (12, 18, 21). Clearly, however, net negative charge was not the sole determinant of activity, because some residues were more critical than others. For instance, the E59A mutation reduced activity further than the E78A mutation did, and activity was lower with E34A/E43A mutations than with E75A/D76A mutations. These results indicate that the transcriptional activity is dependent not only on the net negative charge but also on the position of the acidic residue in the WSSV IE1 TAD. To explain why some acidic residues might be more important than others, we note that acidic activators interact with general transcription factors such as transcription factor IIB and TATA-box binding protein (3, 25, 45), and we further note that in the case of the TAD of



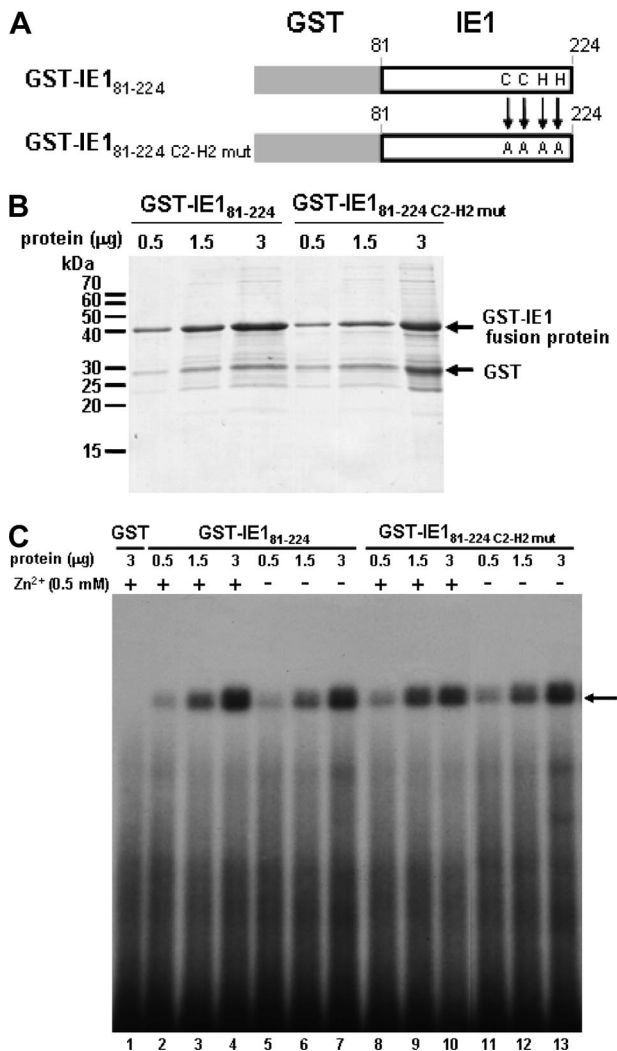


FIG. 5. The DNA binding domain of IE1 is located in the C terminus, and the putative zinc finger motif is not essential for DNA binding. (A) Schematic representation of the GST-IE1 fusion proteins used for the EMSA reaction. In GST-IE1<sub>81-224</sub>, the IE1 N-terminal TAD was deleted; in GST-IE1<sub>81-224</sub>C2-H2mut, the cysteine and histidine residues in the putative zinc finger motif were also replaced by alanine. (B) SDS-PAGE analysis of the purified proteins used for EMSA reactions. (C) DNA binding properties of the IE1 N-terminally truncated fusion proteins. Both GST-IE1<sub>81-224</sub> (0.5 to 3 μg) and GST-IE1<sub>81-224</sub> C2-H2mut (0.5 to 3 μg) were detected by EMSA, regardless of whether Zn ions were present in the DNA binding buffer. The arrows indicate the protein-DNA complexes.

HSV VP16, one specific acidic residue (E476) was shown to be the most important residue for this transactivator's interaction with the human general cofactor PC4 (25). Since IE1 also presumably interacts with various factors and cofactors, we therefore hypothesize that each of these interactions is likewise mediated by specific acidic residues. Alternatively, it is also possible that mutation of the acidic amino acids in IE1's TAD may diminish IE1's activity by disrupting its secondary structure, as shown for other transcription factors (13, 48).

In the region of the TAD (aa 1 to 80) of WSSV IE1, three possible inhibitory domains were identified, at aa 41 to 49, aa 81 to 92, and aa 93 to 137. To date, little is known about

sequences which mediate transcription inhibition and which are present within transcriptional activators. We note, however, that the WSSV IE1 potential inhibitory domain from aa 41 to 49 contains a large proportion of positively charged amino acids (GIEVMKRRL [the three basic residues are underlined]). Slack and Blissard (50) suggested that the substantial concentrations of positively charged amino acids in two inhibition domains of the baculovirus AcMNPV IE1 may act to neutralize the adjacent activation region. It is possible that the basic amino acids in WSSV IE1 aa 41 to 49 are likewise responsible for negatively regulating WSSV IE1's transcriptional activation. The putative WSSV IE1 inhibitory domains at aa 81 to 92 and aa 93 to 137 do not contain large proportions of basic residues. If they regulate the TAD activity, it is therefore probable that they do so either by direct interactions with components of the general transcription factors (4, 51) or by indirect interactions through secondary "inhibitor" proteins that mask the activation domain (2, 5).

In addition to the TAD, most transcriptional factors also require a second region that confers specificity for target genes. This region may confer target gene specificity either directly (in the form of a DBD) or indirectly (by serving as an interface for protein-protein interactions with factors bound to target genes). Our EMSA results (Fig. 5C) suggested that IE1 has a DBD in the C terminus, and a previous amino acid sequence analysis of this region identified a putative classic zinc finger Cys<sub>2</sub>/His<sub>2</sub> domain between aa 186 and 215 (31). When this zinc finger motif was mutated, however, the mutant protein still retained its ability to bind DNA, and the absence of Zn<sup>2+</sup> failed to impair this ability (Fig. 5C, lanes 8 to 10 and 11 to 13). We therefore concluded that IE1's putative zinc finger motif cannot be directly responsible for its DNA binding activity. In further support of this conclusion, we also note that classic zinc finger motifs usually contain a compact ββα structure (27, 41, 43, 58), but the predicted secondary structure of the WSSV IE1 zinc finger motif obtained using the NNpredict, SOPMA, JPRED, and PHD programs (<http://ca.expasy.org/tools/>) does not contain this conserved structure (data not shown).

When there is only a single predicted zinc finger in a transcription factor (for example, human cytomegalovirus immediate-early protein IE2 [1]), it is not always used to bind DNA. On the contrary, when transcription factors use zinc fingers to bind DNA, there are usually several (often three or more) fingers involved (24, 36, 58). Furthermore, the involvement of zinc finger motifs in other activities has also been documented for viruses. For instance, the herpesvirus saimiri immediate-early protein ORF57 is a transcriptional activator with a zinc finger-like domain in its C terminus, and during a herpesvirus saimiri infection, this domain is required for transactivation, repression of viral proteins, and the redistribution of the host splicing factor SC-35 (19). Other examples include adenovirus E1A, which has a zinc finger domain that functions in protein-protein interactions and transactivation activity (17, 47), and HSV type 1 immediate-early protein ICP27, whose C-terminal zinc finger domain is required for ICP27 self-interaction (61).

In the case of IE1, several observations are relevant to the possible function of its zinc finger. Like many other virus immediate-early proteins that bind DNA in a dimeric form (8, 16, 40, 57), our evidence suggests that WSSV IE1 also has this

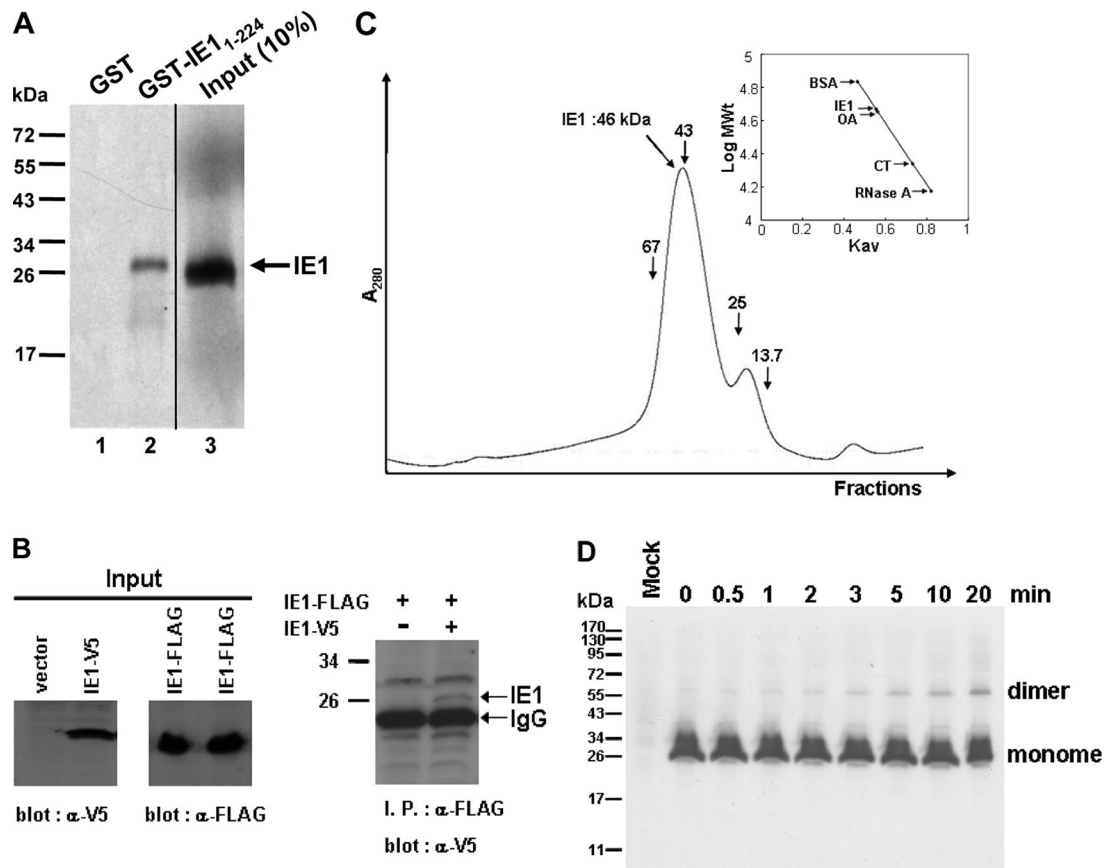


FIG. 6. Homotypic interaction and dimerization of IE1. (A) SDS-PAGE analysis showing the reaction of GST-IE1 fusion protein with [<sup>35</sup>S]methionine-labeled IE1 protein (input). The full-length IE1 protein is indicated by the arrow. (B) Self-interaction of IE1 demonstrated by coimmunoprecipitation. V5-tagged IE1 was transiently coexpressed in Sf9 cells with FLAG-tagged IE1. Six hours after being heat shocked, the cell lysates were harvested and immunoprecipitated with anti-FLAG M2 affinity resins. The immunoprecipitated complexes were then subjected to Western blot analysis with anti-V5 antibody. The detected V5-tagged IE1 is indicated by the arrow. The two panels on the left show the FLAG- and V5-tagged IE1 inputs. (C) Size exclusion chromatography of IE1 on a Superdex 200-pg gel filtration column monitored at 280 nm. The protein standards bovine serum albumin (BSA; 67 kDa), ovalbumin (OA; 43 kDa), chymotrypsinogen A (CT; 25 kDa), and RNase A (13.7 kDa) were fractionated on the same column. The inset shows a plot of the  $K_{av}$  for each protein against the logarithm of its molecular size (log MWt). (D) Kinetic study of glutaraldehyde cross-linking of IE1 expressed in Sf9 cells. Transiently expressed V5-tagged IE1 was treated with 0.01% glutaraldehyde for the indicated times at room temperature and subjected to Western blotting with anti-IE1 antibody. Mock, transfection with vector plasmid.

characteristic. Starting from the EMSA results (Fig. 4B and 5C), the presence of only a single band of IE1-DNA complex suggests that only a single form of IE1 was involved in DNA binding. This single form was most likely the IE1 homodimer, because when the same purified IE1<sub>1-224</sub> construct that was used for Fig. 4B was subjected to gel filtration chromatography, IE1's apparent molecular size was 46 kDa (i.e., approximately double the predicted molecular size of the IE1 monomer [~25 kDa]). IE1's ability to self-interact is also supported by the GST pull-down and coimmunoprecipitation data (Fig. 6A and B) and by the glutaraldehyde cross-linking analysis (Fig. 6D). Thus, it is possible that, as in ICP27 (61), the putative zinc finger motif of WSSV IE1 may be involved in the formation of the IE1 homodimer. More work will be needed to investigate this possibility and to elucidate the mechanisms involved.

In conclusion, we have been able to ascribe several functions to separate regions of the WSSV IE1 protein. Our data suggest that WSSV IE1 has at least two distinguishable domains, an

N-terminal region that is essential for transactivation and a C-terminal region that is required for DNA binding activity. We also conclude that IE1 probably occurs primarily as a homodimeric protein.

#### ACKNOWLEDGMENTS

This investigation was supported financially by a National Science Council grant (NSC96-2317-B-002-005) and by the Council of Agriculture (97AS-14.1.1-AQ-B1).

We are indebted to Paul Barlow for his helpful criticism.

#### REFERENCES

- Asmar, J., L. Wiebusch, M. Truss, and C. Hagemeier. 2004. The putative zinc finger of the human cytomegalovirus IE2 86-kilodalton protein is dispensable for DNA binding and autorepression, thereby demarcating a concise core domain in the C terminus of the protein. *J. Virol.* **78**:11853-11864.
- Baichwal, V. R., A. Park, and R. Tjian. 1992. The cell-type-specific activator region of c-Jun juxtaposes constitutive and negatively regulated domains. *Genes Dev.* **6**:1493-1502.
- Blair, W. S., H. P. Bogerd, S. J. Madore, and B. R. Cullen. 1994. Mutational analysis of the transcription activation domain of RelA: identification of a highly synergistic minimal acidic activation module. *Mol. Cell. Biol.* **14**:7226-7234.

4. Boyd, J. M., P. M. Loewenstein, Q. Tang, L. Yu, and M. Green. 2002. Adenovirus E1A N-terminal amino acid sequence requirements for repression of transcription in vitro and in vivo correlate with those required for E1A interference with TBP-TATA complex formation. *J. Virol.* **76**:1461–1474.
5. Brown, H. J., J. A. Sutherland, A. Cook, A. J. Bannister, and T. Kouzarides. 1995. An inhibitor domain in c-Fos regulates activation domains containing the HOB1 motif. *EMBO J.* **14**:124–131.
6. Buczynski, K. A., S. K. Kim, and D. J. O'Callaghan. 1999. Characterization of the transactivation domain of the equine herpesvirus type 1 immediate-early protein. *Virus Res.* **65**:131–140.
7. Chen, L.-L., H.-C. Wang, C.-J. Huang, S.-E. Peng, Y.-G. Chen, S.-J. Lin, W.-Y. Chen, C.-F. Dai, H.-T. Yu, C.-H. Wang, C.-F. Lo, and G.-H. Kou. 2002. Transcriptional analysis of the DNA polymerase gene of shrimp white spot syndrome virus. *Virology* **301**:136–147.
8. Chiou, C.-J., J. Zong, I. Waheed, and G. S. Hayward. 1993. Identification and mapping of dimerization and DNA-binding domains in the C terminus of the IE2 regulatory protein of human cytomegalovirus. *J. Virol.* **67**:6201–6214.
9. Choi, Y.-S., and S. Sinha. 2006. Determination of the consensus DNA-binding sequence and a transcriptional activation domain for ESE-2. *Biochem. J.* **398**:497–507.
10. Chou, H.-Y., C.-Y. Huang, C.-H. Wang, H.-C. Chiang, and C.-F. Lo. 1995. Pathogenicity of a baculovirus infection causing white spot syndrome in cultured penaeid shrimp in Taiwan. *Dis. Aquat. Organ.* **23**:165–173.
11. Courey, A. J., D. A. Holtzman, S. P. Jackson, and R. Tjian. 1989. Synergistic activation by the glutamine-rich domains of human transcription factor Sp1. *Cell* **59**:827–836.
12. Cress, W. D., and S. J. Triezenberg. 1991. Critical structural elements of the VP16 transcriptional activation domain. *Science* **251**:87–90.
13. Defosse, P. A., J. L. Baert, M. Monnot, and Y. de Launoit. 1997. The ETS family member ERM contains an alpha-helical acidic activation domain that contacts TAFII60. *Nucleic Acids Res.* **25**:4455–4463.
14. Flegel, T. W. 1997. Special topic review: major viral diseases of the black tiger prawn (*Penaeus monodon*) in Thailand. *World J. Microbiol. Biotech.* **13**:422–433.
15. Forsythe, I. J., C. E. Shippam, L. G. Willis, S. Stewart, T. Grigliatti, and D. A. Theilmann. 1998. Characterization of the acidic domain of the IE1 regulatory protein from *Oryza pseudotsugata* multicapsid nucleopolyhedrovirus. *Virology* **252**:65–81.
16. Gallinari, P., K. Wiebauer, M. C. Nardi, and J. Jiricny. 1994. Localization of a 34-amino-acid segment implicated in dimerization of the herpes simplex virus type 1 ICP4 polypeptide by a dimerization trap. *J. Virol.* **68**:3809–3820.
17. Geisberg, J. V., W. S. Lee, A. J. Berk, and R. P. Ricciardi. 1994. The zinc finger region of the adenovirus E1A transactivating domain complexes with the TATA box binding protein. *Proc. Natl. Acad. Sci. USA* **91**:2488–2492.
18. Gill, G., and M. Ptashne. 1987. Mutants of GAL4 protein altered in an activation function. *Cell* **51**:121–126.
19. Goodwin, D. J., K. T. Hall, M. S. Giles, M. A. Calderwood, A. F. Markham, and A. Whitehouse. 2000. The carboxy terminus of the herpesvirus saimiri ORF 57 gene contains domains that are required for transactivation and transrepression. *J. Gen. Virol.* **81**:2253–2265.
20. Hemsley, A., N. Arnheim, M. D. Toney, G. Cortopassi, and D. J. Galas. 1989. A simple method for site-directed mutagenesis using the polymerase chain reaction. *Nucleic Acids Res.* **17**:6545–6551.
21. Hope, I. A., S. Mahadevan, and K. Struhl. 1988. Structural and functional characterization of the short acidic transcriptional activation region of yeast GCN4 protein. *Nature* **333**:635–640.
22. Hossain, M. S., S. Khadjjah, and J. Kwang. 2004. Characterization of ORF89—a latency-related gene of white spot syndrome virus. *Virology* **325**:106–115.
23. Inouye, K., S. Miwa, N. Oseko, H. Nakano, and T. Kimura. 1994. Mass mortalities of cultured kuruma shrimp, *Penaeus japonicus*, in Japan in 1993: electron microscopic evidence of the causative virus. *Fish Pathol.* **29**:149–158.
24. Iuchi, S. 2001. Three classes of C<sub>2</sub>H<sub>2</sub> zinc finger proteins. *Cell. Mol. Life Sci.* **58**:625–635.
25. Jonker, H. R., R. W. Wechselberger, R. Boelens, G. E. Folkers, and R. Kaptein. 2005. Structural properties of the promiscuous VP16 activation domain. *Biochemistry* **44**:827–839.
26. Kovacs, G. R., J. Choi, L. A. Guarino, and M. D. Summers. 1992. Functional dissection of the *Autographa californica* nuclear polyhedrosis virus immediate-early 1 transcriptional regulatory protein. *J. Virol.* **66**:7429–7437.
27. Lee, M. S., G. P. Gippert, K. V. Soman, D. A. Case, and P. E. Wright. 1989. Three-dimensional solution structure of a single zinc finger DNA-binding domain. *Science* **245**:635–637.
28. Leu, J.-H., Y.-C. Kuo, G.-H. Kou, and C.-F. Lo. 2008. Molecular cloning and characterization of an inhibitor of apoptosis protein (IAP) from the tiger shrimp, *Penaeus monodon*. *Dev. Comp. Immunol.* **32**:121–133.
29. Lin, Y.-S., M. Carey, M. Ptashne, and M. R. Green. 1990. How different eukaryotic transcriptional activators can cooperate promiscuously. *Nature* **345**:359–361.
30. Liu, W.-J., Y.-S. Chang, A. H.-J. Wang, G.-H. Kou, and C.-F. Lo. 2007. White spot syndrome virus annexes a shrimp STAT to enhance expression of the immediate-early gene *iel*. *J. Virol.* **81**:1461–1471.
31. Liu, W.-J., Y.-S. Chang, C.-H. Wang, G.-H. Kou, and C.-F. Lo. 2005. Microarray and RT-PCR screening for white spot syndrome virus immediate-early genes in cycloheximide-treated shrimp. *Virology* **334**:327–341.
32. Lo, C.-F., C.-H. Ho, C.-H. Chen, K.-F. Liu, Y.-L. Chiu, P.-Y. Yeh, S.-E. Peng, H.-C. Hsu, H.-C. Liu, C.-F. Chang, M.-S. Su, C.-H. Wang, and G.-H. Kou. 1997. Detection and tissue tropism of white spot syndrome baculovirus (WSBV) in captured brooders of *Penaeus monodon* with a special emphasis on reproductive organs. *Dis. Aquat. Organ.* **30**:53–72.
33. Lo, C.-F., C.-H. Ho, S.-E. Peng, C.-H. Chen, H.-C. Hsu, Y.-L. Chiu, C.-F. Chang, K.-F. Liu, M.-S. Su, C.-H. Wang, and G.-H. Kou. 1996. White spot syndrome baculovirus (WSBV) detected in cultured and captured shrimp, crabs and other arthropods. *Dis. Aquat. Organ.* **27**:215–225.
34. Lu, L., H. Wang, I. Manoppo, L. Yu, and J. Kwang. 2005. Baculovirus-mediated promoter assay and transcriptional analysis of white spot syndrome virus *orf427* gene. *Virol. J.* **2**:71. <http://www.virologyj.com/content/2/1/71>.
35. Massari, M. E., and C. Murre. 2000. Helix-loop-helix proteins: regulators of transcription in eucaryotic organisms. *Mol. Cell. Biol.* **20**:429–440.
36. McDowall, J. 2007. Protein of the month: zinc fingers. [http://www.ebi.ac.uk/interpro/potm/2007\\_3/Page1.htm](http://www.ebi.ac.uk/interpro/potm/2007_3/Page1.htm).
37. Mermod, N., E. A. O'Neill, T. J. Kelly, and R. Tjian. 1989. The proline-rich transcriptional activator of CTF/NF-1 is distinct from the replication and DNA binding domain. *Cell* **58**:741–753.
38. Momoyama, K., M. Hiraoka, H. Nakano, H. Koube, K. Inouye, and N. Oseko. 1994. Mass mortalities of cultured kuruma shrimp, *Penaeus japonicus*, in Japan in 1993: histopathological study. *Fish Pathol.* **29**:141–148.
39. Nakano, H., H. Koube, S. Umezawa, K. Momoyama, M. Hiraoka, K. Inouye, and N. Oseko. 1994. Mass mortalities of cultured kuruma shrimp, *Penaeus japonicus*, in Japan in 1993: epizootiological survey and infection trails. *Fish Pathol.* **29**:135–139.
40. Olson, V. A., J. A. Wetter, and P. D. Friesen. 2003. The highly conserved basic domain I of baculovirus IE1 is required for *hr* enhancer DNA binding and *hr*-dependent transactivation. *J. Virol.* **77**:5668–5677.
41. Parraga, G., S. J. Horvath, A. Eisen, W. E. Taylor, L. Hood, E. T. Young, and R. E. Klevit. 1988. Zinc-dependent structure of a single-finger domain of yeast ADRI. *Science* **241**:1489–1492.
42. Patikoglou, G., and S. K. Burley. 1997. Eukaryotic transcription factor-DNA complexes. *Annu. Rev. Biophys. Biomol. Struct.* **26**:289–325.
43. Pavletich, N. P., and C. O. Pabo. 1991. Zinc finger-DNA recognition: crystal structure of a Zif268-DNA complex at 2.1 Å. *Science* **252**:809–817.
44. Regier, J. L., F. Shen, and S. J. Triezenberg. 1993. Pattern of aromatic and hydrophobic amino acids critical for one of two subdomains of the VP16 transcriptional activator. *Proc. Natl. Acad. Sci. USA* **90**:883–887.
45. Roberts, S. G., I. Ha, E. Maldonado, D. Reinberg, and M. R. Green. 1993. Interaction between an acidic activator and transcription factor TFIIB is required for transcriptional activation. *Nature* **363**:741–744.
46. Sadowski, L., J. Ma, S. Triezenberg, and M. Ptashne. 1988. GAL4-VP16 is an unusually potent transcriptional activator. *Nature* **335**:563–564.
47. Sanchez, T. A., I. Habib, J. L. Booth, S. M. Everts, and J. P. Metcalf. 2000. Zinc finger and carboxyl regions of adenovirus E1A 13S CR3 are important for transactivation of the cytomegalovirus major immediate early promoter by adenovirus. *Am. J. Respir. Cell Mol. Biol.* **23**:670–677.
48. Schmitz, M. L., M. A. dos Santos Silva, H. Altmann, M. Czisch, T. A. Holak, and P. A. Baeuerle. 1994. Structural and functional analysis of the NF-kappa B p65 C terminus. An acidic and modular transactivation domain with the potential to adopt an alpha-helical conformation. *J. Biol. Chem.* **269**:25613–25620.
49. Sekimata, M., and Y. Homma. 2004. Sequence-specific transcriptional repression by an MBD2-interacting zinc finger protein MIZF. *Nucleic Acids Res.* **32**:590–597.
50. Slack, J. M., and G. W. Blissard. 1997. Identification of two independent transcriptional activation domains in the *Autographa californica* multicapsid nuclear polyhedrosis virus IE1 protein. *J. Virol.* **71**:9579–9587.
51. Song, C.-Z., P. M. Loewenstein, K. Toth, and M. Green. 1995. Transcription factor TFIID is a direct functional target of the adenovirus E1A transcription-repression domain. *Proc. Natl. Acad. Sci. USA* **92**:10330–10333.
52. Stenberg, R. M. 1996. The human cytomegalovirus major immediate-early gene. *Intervirology* **39**:343–349.
53. Takahashi, Y., T. Itami, M. Kondo, M. Maeda, R. Fujii, S. Tomonaga, K. Supamattaya, and S. Boonyaratpalin. 1994. Electron microscopic evidence of bacilliform virus infection in kuruma shrimp (*Penaeus japonicus*). *Fish Pathol.* **29**:121–125.
54. Triezenberg, S. J. 1995. Structure and function of transcriptional activation domains. *Curr. Opin. Gen. Dev.* **5**:190–196.
55. van Hulten, M. C. W., J. Witteveldt, S. Peters, N. Kloosterboer, R. Tarchini, M. Fiers, H. Sandbrink, R. K. Lankhorst, and J. M. Vlak. 2001. The white spot syndrome virus DNA genome sequence. *Virology* **286**:7–22.
56. Vlak, J. M., J. R. Bonami, T. W. Flegel, G.-H. Kou, D. V. Lightner, C.-F. Lo, P. C. Loh, and P. J. Walker. 2004. *Nimaviridae*, p. 187–192. *In* C. M. Fauquet, M. A. Mayo, J. Maniloff, U. Desselberger, and L. A. Ball (ed.), VIIIth report

- of the International Committee on Taxonomy of Viruses. Elsevier, Amsterdam, The Netherlands.
57. **West, J. T., and C. Wood.** 2003. The role of Kaposi's sarcoma-associated herpesvirus/human herpesvirus-8 regulator of transcription activation (RTA) in control of gene expression. *Oncogene* **22**:5150–5163.
  58. **Wolfe, S. A., L. Nekludova, and C. O. Pabo.** 2000. DNA recognition by Cys2His2 zinc finger proteins. *Annu. Rev. Biophys. Biomol. Struct.* **29**:183–212.
  59. **Wongteerasupaya, C., J. E. Vickers, S. Sriurairatana, G. L. Nash, A. Akarajamorn, V. Boosaeng, S. Panyim, A. Tassanakajon, B. Withyachumnarnkul, and T. W. Flegel.** 1995. A non-occluded, systemic baculovirus that occurs in the cells of ectodermal and mesodermal origin and causes high mortality in the black tiger prawn *Penaeus monodon*. *Dis. Aquat. Organ.* **21**:69–77.
  60. **Yang, F., J. He, X. Lin, Q. Li, D. Pan, X. Zhang, and X. Xu.** 2001. Complete genome sequence of the shrimp white spot bacilliform virus. *J. Virol.* **75**:11811–11820.
  61. **Zhi, Y., K. S. Sciabica, and R. M. Sandri-Goldin.** 1999. Self-interaction of the herpes simplex virus type 1 regulatory protein ICP27. *Virology* **257**:341–351.